SCIENTIFIC REPORTS

OPEN

SUBJECT AREAS:
NUCLEIC ACIDS
ORGANIZING MATERIALS WITH DNA

Received
28 May 2014

Accepted
8 July 2014

Published
4 August 2014

Correspondence and requests for materials should be addressed to F.X. (xiafan@hust.edu.cn)

* These authors contributed equally to this work.

Imparting biomolecules to a metal-organic framework material by controlled DNA tetrahedron encapsulation

Yongmei Jia[1]*, Benmei Wei[1]*, Ruixue Duan[1], Ying Zhang[1], Boya Wang[1], Abdul Hakeem[1], Nannan Liu[1], Xiaowen Ou[1], Shaofang Xu[1], Zhifei Chen[1], Xiaoding Lou[1] & Fan Xia[1,2]

[1]Key Laboratory for Large-Format Battery Materials and System, Ministry of Education, School of Chemistry and Chemical Engineering, Huazhong University of Science and Technology, Wuhan 430074, China, [2]National Engineering Research Center for Nanomedicine, Huazhong University of Science and Technology, Wuhan 430074, China.

Recently, the incorporation of biomolecules in Metal-organic frameworks (MOFs) attracts many attentions because of controlling the functions, properties and stability of trapped molecules. Although there are few reports on protein/MOFs composites and their applications, none of DNA/MOFs composite is reported, as far as we know. Here, we report a new composite material which is self-assembled from 3D DNA (guest) and pre-synthesized MOFs (host) by electrostatic interactions and hydrophilic interactions in a well-dispersed fashion. Its biophysical characterization is well analyzed by fluorescence spectroscopy, quartz crystal microbalance (QCM) and transmission electron microscopy (TEM). This new composite material keeps 3D DNA nanostructure more stable than only 3D DNA nanostructure in DI water at room temperature, and stores amounts of genetic information. It will make DNA as a guest for MOFs and MOFs become a new platform for the development of DNA nanotechnology.

Metal-organic frameworks (MOFs) are permanently microporous materials synthesized by assembling metal ions with organic ligands in appropriate solvents[1–4]. They have crystalline structures and typically are characterized by large internal surface areas, uniform but tunable cavities and tailorable chemistry[5,6]. Their porous crystals are useful because they allow access of molecules through their pore apertures for gas storage, chemical separation[7–9], catalysis[10,11], drug delivery[12–15] and sensing[16–18]. The pore apertures dictate the size of the molecules that may enter the pores, which provide the surface and space to carry out these functions[19–22]. By serving as unique host matrices for various functional species, they also offer the opportunity to develop new types of composite materials that display enhanced (gas storage) or new (catalytic, optical and electrically conductive) behaviors in comparison to the parent MOFs counterparts[2,23].

In particular, the incorporation of biomolecules in MOFs attracts much attention because of controlling the functions, properties and stability of the trapped molecules. Biomolecule/MOFs composites can be prepared either by using MOFs as templates to generate biomolecules within their cavities or by encapsulating pre-synthesized biomolecules in MOFs. In the former case, small and naked biomolecules are generated and embedded in the cavities of MOFs. In the latter, however, usually the biomolecules are stabilized with certain surfactants, capping agents or even ions, and the biomolecules hydrodynamic radius are much larger than the cavity size of MOFs. The biomolecules do not occupy the MOFs cavities, but instead are surrounded by grown MOFs materials. For example, Fujita et al. utilizes self-assembly to construct sphere frameworks around a covalently tethered protein[24]. The protein was attached to one bidentate ligand and, upon addition of Pd (II) ions (M) and additional ligands (L), $M_{12}L_{24}$ sphere framework self-assembled around the protein. Omar M. Yaghi et al. reports a strategy to expand the pore aperture of MOFs into a previously unattained size regime[3,25]. The pore apertures of IRMOF-74-VII and IRMOF-74-IX are large enough for natural proteins, such as vitamin B12, myoglobin, and green fluorescent protein (GFP) to enter the pores respectively.

Although there are few reports on protein/MOF composites and their applications (mainly focused on controlling the proteins' structure, making the functional proteins or enhancing protein stability), there are no reported examples of DNA/MOFs composites, as far as we know. This emerging area is characterized by

significant challenges, several of which we address here. First, effective control over the spatial distribution of DNA nanostructure within the MOFs matrix is largely lacking with existing strategies for encapsulation. In addition, the choose and synthesis of a suitable MOFs for DNA encapsulation is a daunting synthetic challenge due to size of DNA, especially 3D DNA nanostructure and the harsh environment of DNA stable existence. Third, the encapsulation of biomolecules will have a significant impact on their chemical properties and should lead to new application, including catalysis, sensing and keeping protein stable. In this regard, the DNA/MOFs composite material seems attractive, but as yet is not developed.

Due to the challenges and potential applications, there have been no reported examples of two dimensional (2D) DNA nanostructures encapsulation by artificial well-defined MOFs, let alone three dimensional (3D) DNA nanostructures[26,27]. Here, we report a new composite material which is self-assembled from 3D DNA (guest) and pre-synthesized MOFs (host) in a well-dispersed fashion by electrostatic interactions and hydrophilic interactions. Its biophysical characterization could be well analyzed by fluorescence spectroscopy, quartz crystal microbalance (QCM) and transmission electron microscopy (TEM). We expect that 3D DNA encapsulation into the MOFs will allow us to explore the function of synthetic hosts for the conformational and functional control of encapsulated 3D DNA. And this new composite material could keep 3D DNA nanostructure more stable than only 3D DNA in DI water at room temperature and store a large amount of genetic information.

Previous studies have proven that 3D DNA nanostructure has excellent mechanical rigidity and structural stability[28–32]. In our work, we choose the DNA tetrahedral nanostructure originally developed by Turberfield et al.[33] as the guest. This tetrahedral nanostructure can be rapidly and reliably assembled by four designed DNA oligonucleotides and easily functionalized with different chemical moieties and biomolecules. Each edge of a tetrahedron is an 18-base-pair double helix, which makes the tetrahedral edges is 5.8 nm in length[34–38]. To meet the require of large size and sensitive nature of DNA, we choose water-insoluble $M_{12}L_{24}$ sphere framework is self-assembled from 12 Pd (II) ions (M) and 24 bent ligands (L) as our first host[39]. We dissolve it in 5% DMSO aqueous solution and detect the interaction between $M_{12}L_{24}$ sphere framework and 3D DNA by QCM. We find that the frequency signal change is due to the effect of DMSO, not because of $M_{12}L_{24}$ effect (Figure S7). Thus, M_6L_4 sphere framework is chosen due to its increased solubility in the aqueous solution mixture. It is a 12+ charged M_6L_4 type sphere framework with a diameter of 7 nm in length, constructed from ten species: 4 bent ligands (L) held together by 6 Pd (II) ions (M). Its tetrahedral symmetry provides a large central void for accommodating 3D DNA due to electron donation to Pd^{2+} centers at three pyridine coordination sites which acts as a strong electron acceptor[22]. M_6L_4 sphere framework is prepared according to the method reported by Fujita et al. Generally, there are three assays to encapsulate DNA tetrahedron into the metal-organic framework. The first assay, aqueous solutions of M_6L_4 sphere frameworks (300 μM, 10 μL), four oligonucleotides (10 μM, 5 μL) and TM buffer (20 μL) are mixed briefly, heated to 95°C for 2 min and immediately cooled to 4°C in about 50 s using a PCR machine and then kept at room temperature for 48 h without stirring. But the reaction forms many precipitates during the self-assemble process of M_6L_4 sphere frameworks and DNA tetrahedrons, which indicates that the M_6L_4 sphere frameworks structure are inevitably collapsed at 95°C in TM buffer, which indicates the assay is not successful to fabricate composite materials. The second assay, the four stands of DNA oligonucleotides, organic ligands and metallic compounds are mixed in TM buffer, but the organic ligands cannot dissolve in DI water which indicates that this method is negative to the forming of M_6L_4 sphere framework. The third assay, we respectively synthesize 3D DNA and M_6L_4 sphere framework in aqueous solution, and then mix the two kinds of aqueous solution directly. Keep them at room temperature for 48 h without stirring. Finally, we obtain the transparent liquid. So in this work, we choose the third method to get the new composite material.

To investigate whether 3D DNA could bind with the M_6L_4 sphere framework, we use FRET measurements by using fluorescence spectrophotometer (Figure 1a). It can confirm the existence of a fluorescence resonance energy transfer pair from donor to acceptor[40,41]. We encapsulate bisanthracene into M_6L_4 sphere framework to form a new photoactive exciplex (the FRET donor). The DNA tetrahedron is labeled with FAM on an un-hybridized "hinge" base (FL-3D DNA, the FRET acceptor). If they can be attracted by electrostatic interactions, forming a new composite material, the donor-acceptor distance would be less than 10 nm, corresponding FRET efficiencies of approximately 90%. In contrast, if they don't have any interaction, the donor–acceptor distance would be greater than 10 nm, corresponding FRET of less than 5%[34]. As shown in Figure 1b, there is a weak peak at 518 nm of the FL-3D DNA. While, mixing the FL-3D DNA and the photoactive exciplex together, there is a new strong emission at 518 nm. It demonstrates that the donor-acceptor distance less than 10 nm. The FRET measurements show that not only electrostatic attractions but also hydrophilic interactions play important roles in the self-assembling process of FL-3D DNA and M_6L_4 sphere framework.

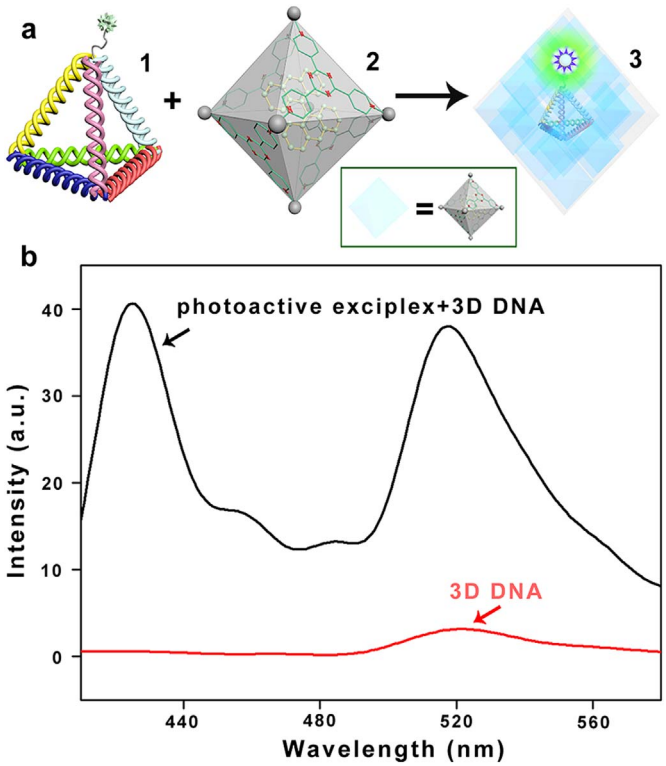

Figure 1 | FRET measurements. (a) Schematic representation of the formation of the proposed composite material Complex 3 from the self-assemble of Complex 1 and 2 by electrostatic interaction. Wherein, complex 1 is the molecular model of a FL-3D DNA formed by annealing of four ssDNA (strands s1-s4 in SI). Complex 2 is the model of metal-organic framework contains bisanthracene. (b) Fluorescence spectra of the Complex 3. The M_6L_4 sphere framework contains bisanthracene (black lane), which significantly enhances the dye (FAM) modified with FL-3D DNA relative to FL-3D DNA alone. It shows that the electrostatic attraction and hydrophilic interaction play important roles in the binding process between DNA tetrahedron and the M_6L_4 sphere framework. All the experiments are incubated at room temperature. The fluorescence spectra are excited at 376 nm.

To test whether the 3D DNA and the M_6L_4 sphere framework can self-assemble to form a new composite material, we design the 3D DNA structure with three thiol groups at three vertices (HS-3D DNA). It can be self-assembled onto Au surfaces by their thiol groups, as monitored in real time by a surface-sensitive acoustic method, quartz crystal microbalance (QCM) (Figure 2a). According to Sauerbrey et al.[42] reports, the change in resonance frequency Δf is proportional to the change of the adsorbed mass Δm. Hence, any adsorption/desorption process at the quartz interface can be monitored. A typical example of a time resolved QCM measurement is shown in Figure 2b. The decrease of frequency is about 100 Hz in 15 minutes, which indicates HS-3D DNA can be anchored at Au surfaces by Au-S chemical bond within 15 minutes, corresponding to the "rapid" phase (Figure 2b red space). Meanwhile, the remaining self-assembled process from B to C takes 3 hours, corresponding to the "slow" process, and the change of frequency is less than 20 Hz in 3 hours, much slower than the first 15 minutes (Figure 2b blue space). When washed by TM buffer (from C point), the frequency keeps almost constant, which indicates that nearly all the HS-3D DNA are assembled onto the Au surface. However, in the presence of M_6L_4 sphere frameworks (from D point), a decrease in resonance frequency is observed, suggesting the adsorption of M_6L_4 sphere frameworks (Figure 2c red space). But addition of more M_6L_4 sphere frameworks doesn't alter the QCM response (from E point to F point). It is mainly due to that the self-assemble process of HS-3D DNA and M_6L_4 sphere frameworks are saturated. Then the system is flushed with TM buffer (from F point). The frequency does not change, which shows that the HS-3D DNA and the M_6L_4 sphere frameworks have strong binding interactions. The QCM results demonstrate that HS-3D DNA and the M_6L_4 sphere framework can self-assemble to form a new stable composite material by electrostatic attractions and hydrophilic interactions.

FRET and QCM results reveal that the 3D DNA and M_6L_4 sphere frameworks are attracted by electrostatic attractions and hydrophilic interactions which can form a stable composite material. When we detect the interaction between $M_{12}L_{24}$ sphere framework and 3D DNA by QCM, the frequency signal change is due to the effect of DMSO, not because of $M_{12}L_{24}$ effect (Figure S7) that indirectly demonstrates that HS-3D DNA is encapsulated into M_6L_4 sphere framework (Figure S8). TEM is utilized to identify whether the DNA tetrahedrons are encapsulated into the M_6L_4 sphere frameworks (Figure 3a). Figure 3b shows TEM images of M_6L_4 sphere frameworks. Because the M_6L_4 sphere framework is translucent stone, light is allowed to penetrate the entire sample, enabling us to systematically section from the top to the bottom. M_6L_4 sphere frameworks are independent but not well distributed in DI water. We find different shapes of the M_6L_4 sphere frameworks according to the TEM images. Some of them are aggregated together, because of the different tilting angles when we take images. Due to the low contrast of DNA nanostructure in TEM test, we label the 5′ end of each strand to form a tetrahedron with AuNPs (5 nm in diameter). Figure 3c is the TEM images of AuNPs modified DNA tetrahedron (AuNPs-3D DNA). According to the images, we can confirm that it is truly the structure of the DNA tetrahedral. Figure 3d is the TEM images of the

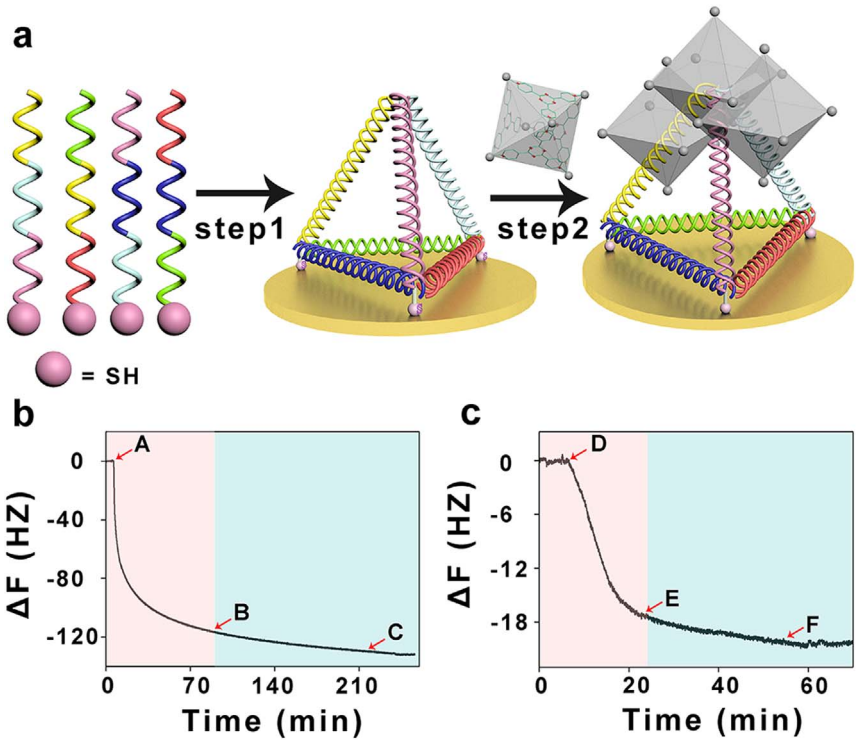

Figure 2 | QCM detection. (a) Schematic representation of the formation of the proposed composite material. Step 1, the HS-3D DNA is expected to readily anchor at the Au surface by Au-S chemical bond. Step 2, M_6L_4 sphere frameworks are expected to be attracted to the platform by electrostatic interaction and hydrophilic interaction. (b) The self-assemble process of HS-3D DNA at the Au surface is monitored in real-time using QCM. It can be anchored at Au surfaces by Au-S chemical bond within 15 minutes, corresponding to the "rapid" process (red space). Meanwhile, the remaining self-assembled process from B to C takes 3 hours, corresponding to the "slow" process, and the change of frequency is less than 20 Hz in 3 hours, much slower than the first 15 minutes, corresponding to the "slow" process (blue space). It indicates that most of the HS-3D DNA are assembled on the Au surface. (c) The self-assemble process of DNA tetrahedrons and M_6L_4 sphere frameworks is monitored in real-time using QCM. In the presence of M_6L_4 sphere frameworks, a decrease in resonance frequency is observed, suggesting the adsorption of M_6L_4 sphere frameworks (red space). Then the self-assemble process is saturated (from E point to F point). But when the system is flushed with TM buffer (from F point to the end), the frequency does not change, which shows that the HS-3D DNA and the M_6L_4 sphere frameworks have strong binding interactions. All the experiments are carried out at room temperature.

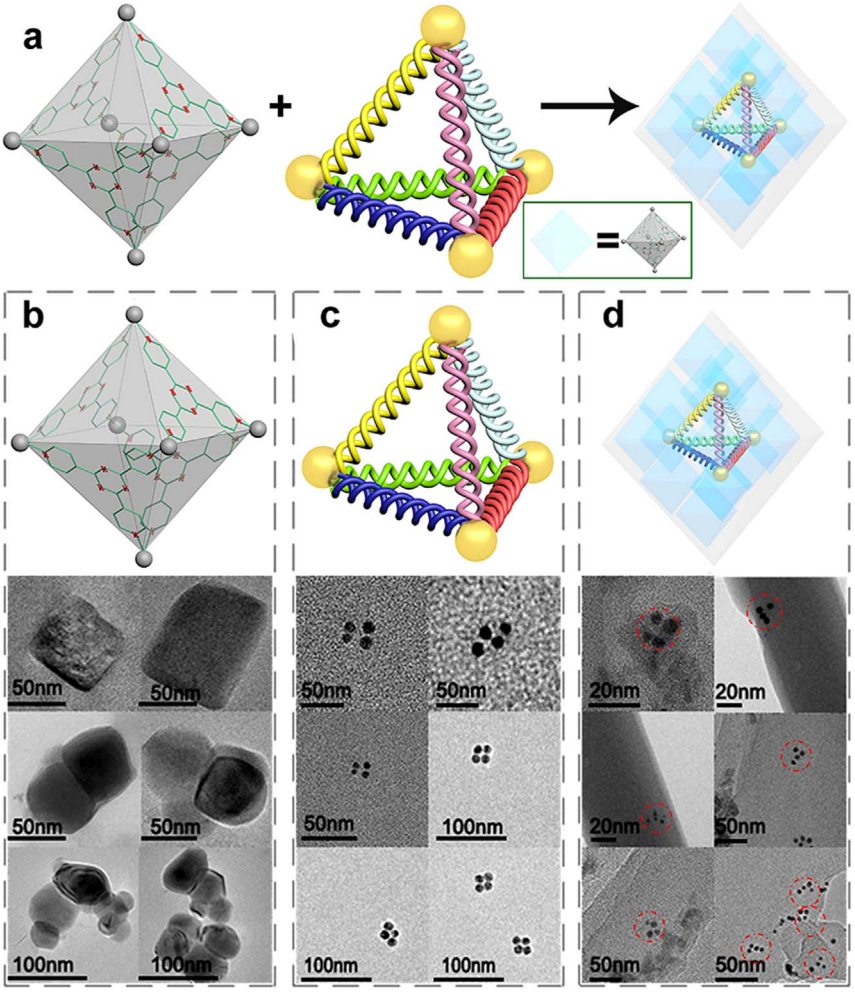

Figure 3 | TEM analysis. (a) Schematic illustration of the forming of the composite material for TEM testing. (b) TEM images of M_6L_4 sphere frameworks. Due to the M_6L_4 sphere frameworks are not well distributed in DI water and the different tilting angles when we take images. We find different shapes of the M_6L_4 sphere frameworks. (c) TEM images of AuNPs modified DNA tetrahedral (AuNPs-3D DNA). Because of the low contrast of DNA nanostructure in TEM test, we label the 5′ end of each strand to form a tetrahedron with four AuNPs (5 nm in diameter). According to the images, we can confirm that it is truly the structure of the AuNPs-3D DNA. (d) TEM images of the new composite material. It is obtained by mixing AuNPs-3D DNA buffer solution and M_6L_4 sphere framework aqueous solution, keeping at room temperature for 48 h without stirring. TEM images reveal that multiple M_6L_4 sphere frameworks contain a AuNPs-3D DNA, yet well disperse. All the experiments are carried out at room temperature.

composite material, obtained by mixing AuNPs-3D DNA buffer solution and M_6L_4 sphere framework aqueous solution, keeping at room temperature for 48 h without stirring. TEM images reveal that multiple M_6L_4 sphere frameworks contain a AuNPs-3D DNA, yet well disperse. But according to the images of the composite compounds, we can conclude DNA (SI Figure S11 there is a DNA characteristic absorption peak at 260 nm) tetrahedron still maintains its tetrahedral structure when it is encapsulated into the M_6L_4 sphere frameworks. The red dash dotted lines in the TEM images are to guide readers to quickly observe AuNPs-3D DNA nanostrctures which are encapsulated into the M_6L_4 sphere frameworks. In order to identify that the AuNPs-3D DNA are encapsulated into the M_6L_4 sphere frameworks, we can get information from the attached chart (Figure S13). The red dash dotted line and blue dash dotted line labeled gold nanoparticles are visible in a different plane, which suggests that the AuNPs-3D DNA nanostructure in the red dashed dotted line is the DNA tetrahedral, which is encapsulated into M_6L_4 sphere frameworks. According to TEM images, we fabricate a new composite material consisting the self-assembly of M_6L_4 sphere frameworks and AuNPs-3D DNA.

2D DNA nanostructure cannot be stable in DI water, let alone 3D DNA nanostructure. Given 3D DNA can be encapsulated into M_6L_4 sphere frameworks, this new composite material may be useful for keeping 3D DNA nanostructure stable. To illustrate this, we monitor the frequency signal changes of the composite material and 3D DNA when they are washed by DI water in real-time using QCM. HS-3D DNA is assembled from 3 thiolated DNA fragments and 1 none modified DNA fragment (All of the 4 strands contain 55-nt nucleotides). It can anchor at Au surface by Au-S chemical bond for the 3 thiolated DNA fragments. The HS-3D DNA nanostructure, however, will disassemble when it is washed by DI water due to the weak hydrogen bonding force. The 1 none modified DNA fragment is washed out of the Au surface. So there is about 25% (1 out of 4 strands) frequency increase. Just as Figure 4 shown, when HS-3D DNA which is layered at Au surface (Figure 4 red space, black line) is washed by DI water, the increase of frequency is about 30 Hz in 300 minutes (Figure 4 blue space). The frequency signal change is about 25% relative to 120 Hz (Figure 2b), which indicates that HS-3D DNA nanostructure is disassembled. However, addition of M_6L_4 sphere frameworks and forming a new composite material (Figure 4 red space) is washed by DI water, the frequency keeps almost constant (Figure 4 blue space, red line), which suggests that HS-3D DNA nanostructure is stable. According to the QCM data, we also believe that this new composite material (M_6L_4-3D DNA) can keep 3D DNA

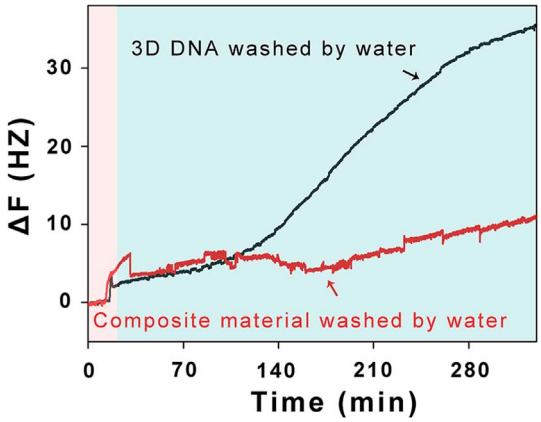

Figure 4 | Apply of composite of material. The 3D DNA nanostructure stable at Au surface is monitored in real-time using QCM. HS-3D DNA nanostructure is synthesized by 3 thiol modified oligonucleotides and 1 none modified oligonucleotide. After HS-3D DNA anchoring at Au surface, the 3 thiol modified oligonucleotides which are anchoring at Au surfaces by Au-S chemical bond can't be washed out of the Au surface by DI water. However, the 1 none modified oligonucleotide could be washed out of the Au surface by DI water. So there is about 25% frequency increase. When HS-3D DNA which is layered at Au surface (black line) is washed by DI water, the increase of frequency is about 30 Hz in 300 minutes (blue space). The frequency signal change is about 25% relative to 120 Hz, which indicates that HS-3D DNA nanostructure is disassembled. However, addition of M_6L_4 sphere frameworks and forming a new composite material is washed by DI water, the frequency keeps almost constant (red line), which suggests that HS-3D DNA nanostructure is stable. The data shows that this new composite material can keep 3D DNA nanostructure more stable than only 3D DNA nanostructure in DI water. All the experiments are carried out at room temperature.

nanostructure more stable than only 3D DNA nanostructure in DI water.

In summary, we successfully synthesize a new composite material which is self-assembled from 3D DNA (guest) and pre-synthesized MOFs (host) by electrostatic attraction and hydrophilic interaction in a well-dispersed fashion. This new composite material can keep 3D DNA nanostructure more stable in DI water than only 3D DNA nanostructure in DI water and store a large amount of genetic information. It will become a general platform in the development of structural DNA nanotechnology. So this composite material will make not only DNA as a guest for the host of MOFs, but also MOFs become a new platform for the development of DNA nanotechnology.

Methods

$M_{12}L_{24}$ sphere framework[39], M_6L_4 sphere framework1 and DNA tetrahedron[28,33] are synthesized according to previous protocol. A detailed description of the protocol can be found in the supporting information.

FRET measurements. A quantity of 100 μL of 1 μM FAM-labeled tetrahedron solution is incubated with 100 μL of 10 μM host-gust exciplex at room temperature for 24 h, and then the solution is directly used for fluorescence. The fluorescence emission spectrum from 410 to 600 nm is measured at 25°C in a quartz cell with 10 mm path length using 376 nm excitation wavelength.

QCM detection. The experimental setup for the QCM-measurements used in the present study is described in more detail elsewhere. Au chip used only for QCM detection is first loaded onto a QCM sensor, and then TM (pH=8.0) solution is pumped into the QCM chamber. After a stable baseline is established, the 3D DNA which is assembled from 3 thiolated DNA fragments and 1 none modified DNA fragment is introduced. The immobilization of DNA on the chip is monitored online. The DNA solution is then replaced by TM buffer, and incubated for 15 min. After a stable baseline is obtained, the metal-organic framework material is introduced and incubates for 60 min, the signal start to decrease and become stable after a certain period of time. Finally, the TM buffer introduce until the baseline smoothly.

Image processing. Mixed the four strands AuNPs modified ssDNA in equimolar quantities in 1×TBE with 50 mM NaCl, heated the mixture to 95°C for 2 min and immediately cooled to 4°C in about 50 s. Then the mixture incubate for 24 h at room temperature to give high yield Au modified DNA tetrahedral.

10 μL solution of the AuNPs Modified DNA tetrahedral is incubated at room temperature in the presence of 100 μL (300 mM) Pd-cage for 1 day. Then the samples are transferred to a copper wire mesh, allowed to dry. Images are collected on a transmission electron microscope at an acceleration voltage of 200 kv.

1. Fujita, M. *et al.* Self-assembly of ten molecules into nanometre-sized organic host frameworks. *Nature* **378**, 469–471 (1995).
2. Lu, G. *et al.* Imparting functionality to a metal–organic framework material by controlled nanoparticle encapsulation. *Nat. Chem.* **4**, 310–316 (2012).
3. Deng, H. *et al.* Multiple Functional Groups of Varying Ratios in Metal-Organic Frameworks. *Science* **327**, 846–850 (2010).
4. Fujita, M., Fujita, N., Ogura, K. & Yamaguchi, K. Spontaneous assembly of ten components into two interlocked, identical coordination cages. *Nature* **400**, 52–55 (1999).
5. Park, Y. K. *et al.* Crystal Structure and Guest Uptake of a Mesoporous Metal–Organic Framework Containing Cages of 3.9 and 4.7 nm in Diameter. *Angew. Chem. Int. Edit.* **46**, 8230–8233 (2007).
6. Hoffman, J. E. *et al.* A Four Unit Cell Periodic Pattern of Quasi-Particle States Surrounding Vortex Cores in $Bi_2Sr_2CaCu_2O_8+\delta$. *Science* **295**, 466–469 (2002).
7. Lee, J. *et al.* Metal-organic framework materials as catalysts. *Chem. Soc. Rev.* **38**, 1450–1459 (2009).
8. Li, J. R. *et al.* Porous materials with pre-designed single-molecule traps for CO2 selective adsorption. *Nat. Commun.* **4**, (2013).
9. Sculley, J. P. & Zhou, H. C. Enhancing Amine-Supported Materials for Ambient Air Capture. *Angew. Chem. Int. Edit.* **51**, 12660–12661 (2012).
10. Park, J. *et al.* A versatile metal-organic framework for carbon dioxide capture and cooperative catalysis. *Chem. Commun.* **48**, 9995–9997 (2012).
11. Du, D. Y. *et al.* An unprecedented (3,4,24)-connected heteropolyoxozincate organic framework as heterogeneous crystalline Lewis acid catalyst for biodiesel production. *Sci Rep.* **3**, (2013).
12. Horcajada, P. *et al.* Porous metal-organic-framework nanoscale carriers as a potential platform for drug delivery and imaging. *Nat. Mater.* **9**, 172–178 (2010).
13. Taylor-Pashow, K. M. L., Rocca, J. D., Xie, Z., Tran, S. & Lin, W. B. Postsynthetic Modifications of Iron-Carboxylate Nanoscale Metal−Organic Frameworks for Imaging and Drug Delivery. *J. Am. Chem. Soc.* **131**, 14261–14263 (2009).
14. McKinlay, A. C. *et al.* BioMOFs: Metal–Organic Frameworks for Biological and Medical Applications. *Angew. Chem. Int. Edit.* **49**, 6260–6266 (2010).
15. Taylor, K. M. L., Rieter, W. J. & Lin, W. B. Manganese-Based Nanoscale Metal−Organic Frameworks for Magnetic Resonance Imaging. *J. Am. Chem. Soc.* **130**, 14358–14359 (2008).
16. Perry, J. J., Bauer, C. A. & Allendorf, M. D. *Luminescent Metal–Organic Frameworks. In Metal-Organic Frameworks: Applications from Catalysis to Gas Storage,* David F., Eds.; *Wiley-VCH Verlag GmbH & Co. KgaA,* 2011; pp 267–308.
17. Lu, G. & Hupp, J. T. Metal−Organic Frameworks as Sensors: A ZIF-8 Based Fabry−Pérot Device as a Selective Sensor for Chemical Vapors and Gases. *J. Am. Chem. Soc.* **132**, 7832–7833 (2010).
18. Feng, D. *et al.* Zirconium-Metalloporphyrin PCN-222: Mesoporous Metal–Organic Frameworks with Ultrahigh Stability as Biomimetic Catalysts. *Angew. Chem. Int. Edit.* **124**, 10453–10456 (2012).
19. Jiang, H. L., Feng, D. W., Liu, T. F., Li, J. R. & Zhou, H. C. Pore Surface Engineering with Controlled Loadings of Functional Groups via Click Chemistry in Highly Stable Metal-Organic Frameworks. *J. Am. Chem. Soc.* **134**, 14690–14693 (2012).
20. Kuo, C.-H. *et al.* Yolk–Shell Nanocrystal@ZIF-8 Nanostructures for Gas-Phase Heterogeneous Catalysis with Selectivity Control *J. Am. Chem. Soc.* **134**, 14345–14348 (2012).
21. Chapman, K. W., Sava, D. F., Halder, G. J., Chupas, P. J. & Nenoff, T. M. Trapping Guests within a Nanoporous Metal–Organic Framework through Pressure-Induced Amorphization. *J. Am. Chem. Soc.* **133**, 18583–18585 (2011).
22. Furutani, Y. *et al.* In Situ Spectroscopic, Electrochemical, and Theoretical Studies of the Photoinduced Host-Guest Electron Transfer that Precedes Unusual Host-Mediated Alkane Photooxidation. *J. Am. Chem. Soc.* **131**, 4764–4768 (2009).
23. Zheng, Y.-R., Lan, W.-J., Wang, M., Cook, T. R. & Stang, P. J. Designed Post-Self-Assembly Structural and Functional Modifications of a Truncated Tetrahedron. *J. Am. Chem. Soc.* **133**, 17045–17055 (2011).
24. Fujita, D. *et al.* Protein encapsulation within synthetic molecular hosts. *Nat. Commun.* **3**, 1093 (2012).
25. Deng, H. *et al.* Large-Pore Apertures in a Series of Metal-Organic Frameworks. *Science* **336**, 1018–1023 (2012).
26. Simmons, C. R. *et al.* Size-Selective Incorporation of DNA Nanocages into Nanoporous Antimony-Doped Tin Oxide Materials. *ACS Nano* **5**, 6060–6068 (2011).
27. Kikuchi, T., Sato, S. & Fujita, M. Well-Defined DNA Nanoparticles Templated by Self-Assembled $M_{12}L_{24}$ Molecular Spheres and Binding of Complementary Oligonucleotides. *J. Am. Chem. Soc.* **132**, 15930–15932 (2010).
28. Goodman, R. P. *et al.* Rapid Chiral Assembly of Rigid DNA Building Blocks for Molecular Nanofabrication. *Science* **310**, 1661–1665 (2005).

29. Pei, H. *et al.* A DNA Nanostructure-based Biomolecular Probe Carrier Platform for Electrochemical Biosensing. *Adv. Mater.* **22**, 4754–4758 (2010).
30. Pei, H. *et al.* Reconfigurable Three-Dimensional DNA Nanostructures for the Construction of Intracellular Logic Sensors. *Angew. Chem. Int. Edit.* **51**, 9020–9024 (2012).
31. Li, J. *et al.* Self-assembled multivalent DNA nanostructures for noninvasive intracellular delivery of immunostimulatory CpG oligonucleotides. *ACS Nano* **5**, 8783–8789 (2011).
32. Shih, W. M., Quispe, J. D. & Joyce, G. F. A 1.7-kilobase single-stranded DNA that folds into a nanoscale octahedron. *Nature* **427**, 618–621 (2004).
33. Goodman, R. P., Berry, R. M. & Turberfield, A. J. The single-step synthesis of a DNA tetrahedron. *Chem. Commun.* 1372–1373 (2004).
34. Flory, J. D. *et al.* PNA-Peptide Assembly in a 3D DNA Nanocage at Room Temperature. *J. Am. Chem. Soc.* **135**, 6985–6993 (2013).
35. Erben, C. M., Goodman, R. P. & Turberfield, A. J. Single-Molecule Protein Encapsulation in a Rigid DNA Cage. *Angew. Chem. Int. Edit.* **45**, 7414–7417 (2006).
36. Modi, S., Nizak, C., Surana, S., Halder, S. & Krishnan, Y. Two DNA nanomachines map pH changes along intersecting endocytic pathways inside the same cell. *Nat. Nanotechnol.* **8**, 459–467 (2013).
37. Shen, X. *et al.* Three-Dimensional Plasmonic Chiral Tetramers Assembled by DNA Origami. *Nano Lett.* **13**, 2128–2133 (2013).
38. Crawford, R. *et al.* Non-covalent Single Transcription Factor Encapsulation Inside a DNA Cage. *Angew. Chem. Int. Edit.* **52**, 2284–2288 (2013).
39. Tominaga, M. *et al.* Finite, Spherical Coordination Networks that Self-Organize from 36 Small Components. *Angew. Chem. Int. Edit.* **43**, 5621–5625 (2004).
40. Murase, T., Nishijima, Y. & Fujita, M. Cage-Catalyzed Knoevenagel Condensation under Neutral Conditions in Water. *J. Am. Chem. Soc.* **134**, 162–164 (2012).
41. Klosterman, J. K., Iwamura, M., Tahara, T. & Fujita, M. Energy Transfer in a Mechanically Trapped Exciplex. *J. Am. Chem. Soc.* **131**, 9478–9479 (2009).
42. Menz, B., Knerr, R., Göpferich, A. & Steinem, C. Impedance and QCM analysis of the protein resistance of self-assembled PEGylated alkanethiol layers on gold. *Biomaterials* **26**, 4237–4243 (2005).

Acknowledgments

This work is supported by initiatory financial support from HUST, National Basic Research Program of China (973 program, 2013CB933000), 1000 Young Talent (to Fan Xia), and the National Natural Science Foundation of China (21375042). The authors thank the HUST Analytical and Testing Center and National Laboratory for Optoelectronics for allowing us to use their facilities. The authors thank Fan Hong and Xihang Liu for drawing the schematic models. The authors thank Jun Su for teaching the use of TEM. The authors also thank Prof. Guochuan Yin for discussing the application of the new DNA/MOF composite material.

Author contributions

Y.M.J., B.M.W. and F.X. designed the study. Y.M.J. performed all chemical synthesis, conducted the FRET, TEM experiments, performed all data analysis and drew all schematic diagrams. B.M.W. conducted the QCM experiment and performed the data analysis. Y.M.J. and F.X. prepared the figures and co-wrote the paper. Y.M.J. and B.M.W. contributed equally to this work. Y.M.J., B.M.W., R.X.D., Y.Z., B.Y.W., A.H., N.N.L., X.W.O., S.F.X., Z.F.C., X.D.L. and F.X. reviewed the manuscript.

Additional information

Supplementary information accompanies this paper at http://www.nature.com/scientificreports

Competing financial interests: The authors declare no competing financial interests.

How to cite this article: Jia, Y. *et al.* Imparting biomolecules to a metal-organic framework material by controlled DNA tetrahedron encapsulation. *Sci. Rep.* **4**, 5929; DOI:10.1038/srep05929 (2014).